Optimization of Hydrothermal Synthesis of Lanthanum-Cobalt Perovskite ($LaCoO_3$): Influence of pH, Stoichiometry, and Sintering Temperature

Vendula Bednaříková[1,*], Michaela Remešová[1], Serhii Tkachenko[1], Martina Vrankić[2], Ladislav Čelko[1]

[1]CEITEC - Central European Institute of Technology, Brno University of Technology, Purkyňova 123, 612 00 Brno, Czech Republic
[2]Division of Materials Physics, Ruđer Bošković Institute, Bijenička cesta 54, 10000 Zagreb, Croatia

Abstract. The aim of this study was to synthesize high-purity $LaCoO_3$ (LCO) using a wet-chemistry hydrothermal route and to systematically evaluate how synthesis parameters affect phase purity and material properties. The effects of the reactant molar ratio, pH, and calcination temperature on the microstructure, morphology, and phase composition of LCO were investigated. Particular attention was given to the formation of the La_2O_3 impurity phase, as even small amounts can significantly influence the physicochemical behaviour of the perovskite. Characterization by powder X-ray diffraction (PXRD), scanning electron microscopy (SEM), and Brunauer-Emmett-Teller (BET) analysis showed that the reactant molar ratio La:Co:citric acid is the most critical factor for reaching phase-pure LCO. Nearly single-phase LCO was achieved at a molar ratio of 1:1.2:1. Calcination at 750 °C resulted in higher phase purity and improved crystallinity as compared to 1150 °C, indicating that excessive temperatures may promote decomposition or impurity phase formation. Furthermore, pH had a significant effect on the final phase composition. A basic pH led preferably to LCO phase formation rather than La_2O_3. Overall, the study demonstrates that careful optimization of reactant ratios, starting mixtures pH, and calcination conditions is essential for obtaining high-purity, nearly single-phase LCO.

1. Introduction

Lanthanum cobaltite ($LaCoO_3$, LCO) is a rare-earth ABO_3 perovskite-type oxide widely studied for its catalytic, magnetic, semiconducting, and oxygen ion-conducting properties [1-5]. Due to its structural flexibility, high chemical and hydrothermal stability, and excellent oxygen mobility, LCO is considered a promising material for catalytic, photocatalytic, and electrochemical applications. The physicochemical properties of LCO strongly depend on the synthesis route, which influences crystallinity, morphology, particle size, surface area, and especially phase purity [6-8]. However, obtaining phase-pure LCO remains challenging because secondary phases, such as La_2O_3 or Co_3O_4, are frequently formed during synthesis.

As recently examined, La_2O_3 impurities enhance cefixime degradation ($k$app = 3.25 × 10^{-3} min^{-1}) as co-catalysts in impurity-modulated LCO samples [9]. Although several studies have reported phase-pure $LaCoO_3$ synthesized via citrate methods [10], sol–gel approaches [11], freeze-drying-assisted precursor routes [12], and hydrothermal methods [13-14], a systematic understanding of the relationship between synthesis conditions and phase evolution is still limited. Therefore, this work investigates the influence of the reactant molar ratio, pH, and calcination temperature on the phase composition and morphology of hydrothermally synthesized $LaCoO_3$ powders.

2. Materials and LCO synthesis

The reactants were purchased commercially and used as received without further purification: lanthanum(III) nitrate hexahydrate ($La(NO_3)_3{\cdot}6\,H_2O$, ≥96%, Merck), cobalt(II) nitrate hexahydrate ($Co(NO_3)_2{\cdot}6\,H_2O$, 99.2%, Lach-ner), citric acid anhydrous ($C_6H_8O_7$, ≥98.5%, Lach-ner), polyethylene glycol 400 (PEG 380-420, Ph.Eur., Roth), ammonium hydroxide solution 24.0% (NH_4OH, 99.2%, Penta), and ethyl alcohol (C_2H_5OH, 99.8%, Lach-ner). The LCO powder samples were synthesized via a citric acid-assisted hydrothermal route as schematically depicted in Figure 1. The $La(NO_3)_3{\cdot}6\,H_2O$ and $Co(NO_3)_2{\cdot}6\,H_2O$ were separately dissolved at room temperature (RT) in demineralized water under vigorous magnetic stirring to prepare 0.5 $mol{\cdot}L^{-1}$ solutions. Citric acid (CA), acting as a chelating agent, was added to the mixed solution, which was then stirred for the next 1 h. The initial pH, measured with a digital pH meter (pHenomenal 1100 L, VWR, USA), was acidic (1.30-

* Corresponding author: Vendula.Bednarikova@ceitec.vutbr.cz

1.60). While maintaining continuous stirring, the pH was gradually adjusted dropwise with ammonium hydroxide solution to 7.05-10.0, depending on the design of the experiment. Immediately after pH adjustment, the mixture was transferred to a 50 mL PTFE-lined stainless-steel autoclave filled to approximately 80 % of its volume, sealed, and heated at 150 ºC for 20 h in a laboratory dryer (SLW-53-W STD, POL-EKO Aparatura, Poland). The autoclave was then allowed to cool naturally to RT. The resulting precipitates were collected by centrifugation, sequentially washed with ethanol and demineralized water, and air-dried at 120 ºC for 12 h. The dried powders were manually ground in an agate mortar and calcined in alumina crucibles under 2 different conditions: (i) 750 ºC for 2 h, and (ii) 1050 ºC for 10 h (LHS 08/15, LAC, Czech Republic) without controlled cooling. The final black LCO powdery samples were collected in vials and stored in a glovebox under an inert N_2 atmosphere to preserve any phase formed during synthesis. Milled precipitates and calcined powders had electrostatic surface charging, which required appropriate handling.

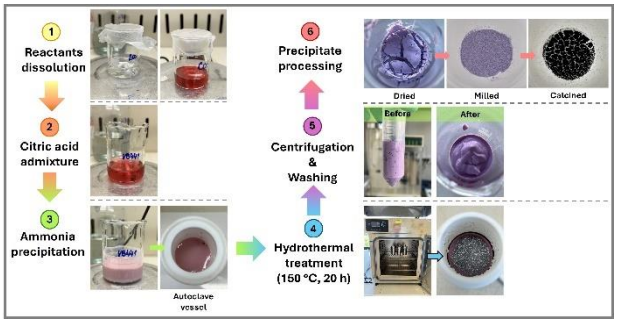

Figure 1. Schematic diagram illustrating the stepwise LCO synthesis.

3. Characterization techniques

The powder X-ray diffraction (PXRD) data at RT were collected in reflection mode with monochromated Cu Kα radiation (λ = 1.54056 Å) on a Rigaku Smartlab 3 kW diffractometer (Rigaku, Japan) operated at 30 mA and 40 kV. Data were collected over a 2θ range of 10–100º with a step size of 0.02º and a scan rate of 3º·min^{-1}. Quantitative phase analysis was performed using the Rietveld method. Surface morphology imaging was performed using a field-emission scanning electron microscope (SEM) Verios 460L (FEI, Czech Republic) operating in immersion mode at an accelerating voltage of 5 kV and a probe current of 0.2 nA. SEM images were obtained using secondary electron (SE) and backscattered electron (BSE) detection modes. To prevent electrostatic charging of the studied powders, a 20 nm thick carbon layer was deposited on their surfaces using the EM ACE600 (Leica Microsystems, Germany).

The specific surface area of the LCO samples was determined from the measured adsorption/desorption isotherms using a Micro 300 C1 surface area analyser (3P Instrument, BET-ANAMET). Prior to measurements, each calcined sample was degassed at 150 ºC for 10 h under vacuum. Nitrogen served as the adsorbate gas, with the bath temperature maintained at liquid nitrogen temperature.

4. Results and discussion

4.1. Hydrothermal synthesis of LCO

LCO samples were successfully synthesized using an autoclave hydrothermal method followed by calcination. In total, 11 samples listed in Table 1 were synthesized in order to obtain a single-phase LCO sample. Basically, 4 experimental conditions were investigated: (i) variation of the molar ratio of reactants, (ii) adjustment of the pH before autoclave treatment, (iii) selection of the calcination temperature in air, (iv) choice of the type of chelating agent. The obtained sample yields and calcination losses are listed in Table 2.

Table 1. Experimental conditions used for LCO samples synthesis.

Sample	La:Co:CA reactant molar ratio*	La:Co: PEG400 reactant molar ratio*	Calcination temperature [°C]	Final pH
LCO1	1:1:1	-	750	8.46
LCO2	1:1:0.5	-	750	8.46
LCO3	1:1:1	-	1050	8.46
LCO4	1:1:1	-	750	10.0
LCO5	1:1:1	-	750	7.05
LCO6	1:1.2:1	-	750	8.50
LCO7	1:1.2:1	-	750	8.51
LCO8	1:1.2:1	-	750	7.96
LCO9	1:1.3:1	-	750	8.49
LCO10	1:1.2:2	-	750	5.70
LCO11	-	1:1:0.005	750	8.27

*reactants: La - $La(NO_3)_3 \cdot 6\ H_2O$;
Co – $Co(NO_3)_2 \cdot 6\ H_2O$, CA - citric acid anhydrous.

Table 2. Summary of yields and calcination losses of synthesized LCO samples.

Sample	Yield after drying [g]	Yield after calcination [g]*	Calcination loss [%]
LCO1	1.7	0.8	45
LCO2	1.2	0.7	40
LCO3	1.8	0.8	45
LCO4	1.1	0.5	36
LCO5	1.6	0.7	51
LCO6	1.9	0.7	57
LCO7	1.9	0.7	57
LCO8	1.9	0.9	44
LCO9	2.0	1.0	43
LCO10	2.0	1.0	45
LCO11	0.65	0.28	29

*major amount of dried sample was used for calcination, a minor amount of sample, approximately 200 mg was stored for further analysis under an inert atmosphere of a glovebox, as their metastability was proved further.

4.2. Phase analysis using X-ray diffraction

Hydrothermally synthesized powders were amorphous; in contrast, the calcined samples exhibit high crystallinity of the detected phases. The summary of quantitative phase analysis obtained from the Rietveld refinement is listed in Table 3.

Table 3. Quantitative phase analysis results of calcinated LCO samples.

Sample	Phase fraction [wt.%]		Sample	Phase fraction [wt.%]	
LCO1	LCO	92.2	**LCO7**	LCO	99.2
	La_2O_3	7.8		La_2O_3	0.8
LCO2	LCO	68.1	**LCO8**	LCO	97.8
	La_2O_3	31.9		La_2O_3	2.2
LCO3	LCO	87.8	**LCO9**	LCO	~ 99.0
	La_2O_3	12.2		La_2O_3	~ 1.0
LCO4	LCO	69.7	**LCO10**	LCO	85.2
	La_2O_3	30.3		La_2O_3	14.8
LCO5	LCO	56.5	**LCO11**	LCO	75.6
	La_2O_3	43.5		La_2O_3	24.4
LCO6	LCO	99.2			
	La_2O_3	0.8			

Examination of the molar ratio effect of citric acid as a chelating agent ranged from 0.5 to 2.0. It was found that the optimum value for synthesizing high-purity LCO is 1.0, corresponding to an equimolar ratio of lanthanum metal salt. In the case of sample LCO10 with a citric acid molar ratio of 2.0, pH adjustment was stopped at a value close to 6, since a further increase in pH either led to dissolution of the precipitate or to precipitation itself. It was also found that the molar ratio of the cobalt reactant significantly affected phase formation. An equimolar ratio of metal salts resulted in up to 90 wt.% LCO phase, while slightly higher Co-salt ratios of 1.2 and 1.3 in samples LCO6, LCO7, and LCO9 produced nearly single-phase compositions. An interesting fact is that, in addition to lanthanum oxide, the sample LCO9 also contained traces of lanthanum carbonate. In addition to the effect of the molar ratio, the hypothesis that cobalt ions could be washed out using demineralized water was examined. The comparative PXRD study of samples LCO6 and LCO7 after 1 and 4 washing cycles, respectively, showed no difference in their phase composition, therefore, the impact of this factor was determined to be insignificant.

Precise pH control of the reaction mixture prior to hydrothermal treatment proved to be an important processing step. LCO samples were synthesized at pH values ranging from 5.7 to 10.0. The lowest pH of 5.7 applied for sample LCO10, in combination with a higher Co ratio, produced 85.2 wt.% of LCO phase. A slightly higher pH of 7 (LCO5), in combination with an equimolar reactant ratio, resulted in the lowest LCO content (56.5 wt.%), while the highest pH of 10 in the LCO4 sample produced 69.7 wt.% of the LCO phase. Based on these results, a pH of 8.5 was found to be optimal for the formation of nearly single-phase LCO perovskite.

A higher calcination temperature of 1050 °C promoted the formation of the lanthanum oxide phase, indicating that the perovskite phase is metastable and transforms into a binary oxidic phase with increasing temperature.

The above-presented results show that citric acid is an effective chelating agent that promotes the formation of nearly single-phase perovskites. Additionally, PEG 400 was used as a neutral agent for its complexation capability in comparison with citric acid. Unlike citric acid, PEG 400 does not provide significant buffering capacity, resulting in a rapid pH increase upon ammonia addition (three drops increased the pH from 3.2 to 7.5, followed by a slower increase to 8.3). PXRD analysis revealed that sample LCO11 contained 75.6 wt.% LCO, indicating that LCO crystal formation is still promoted with this type of chelating agent, although at a lower yield compared to the citric-assisted synthesis. The highest-purity samples synthesized with an excess of Co reactant (LCO6 and LCO7) at pH 8.5 exhibited the largest calcination loss of 57%, which may be related to stronger chelation agent activity and, according to PXRD results, to total combustion.

4.3. Surface morphology using scanning electron microscopy (SEM)

Figure 2 shows micrographs of the LCO samples. The calcined powders exhibit well-developed submicron structures composed of nearly spherical particles with a high pore density. Samples LCO1 and LCO9 show minimal particle agglomeration, whereas LCO3, LCO4,

LCO5, and LCO6 exhibit larger particle aggregates. Sample LCO2 consists of larger particles due to the higher calcination temperature (1050 ºC). Well-defined grain boundaries and multiple junctions were observed in all sample morphologies except LCO4, where grain boundaries are merged.

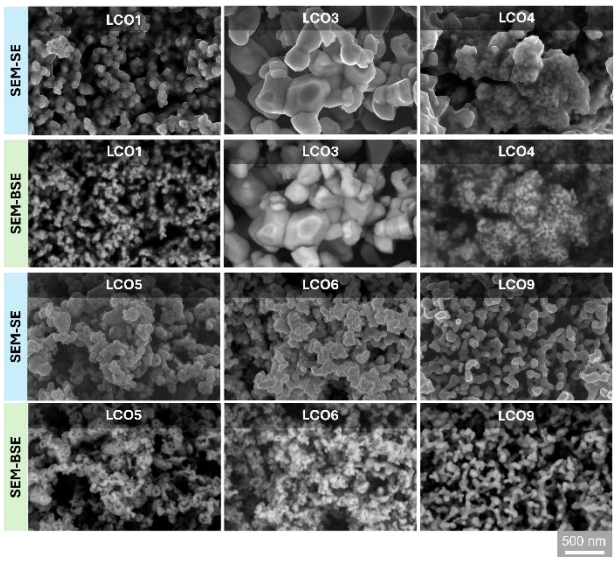

Figure 2. SEM micrographs of LCO samples acquired in SE and BSE imaging modes.

4.4. Brunauer-Emmett-Teller (BET) surface area analysis

Surface area characteristics determined by BET analysis of the selected calcined LCO samples are listed in Table 4. The surface areas ranged from 3.56 to 21.58 m^2/g, with the highest value determined for LCO5 (pH 7, 1:1 La:Co cation ratio). As expected from the SEM and PXRD measurements, LCO3 (calcined at a temperature of 1050 ºC) showed the lowest surface area (3.56 m^2/g) and pore volume (~0.01 cm^3/g). On the other hand, LCO5 and LCO9 exhibited significantly higher surface areas (21.58 and 10.14 m^2/g, respectively) and pore volumes, both several times greater than those of LCO3.

Table 4. Surface area and porosity characteristics of selected calcined LCO samples.

Sample	Surface area [m^2/g]	Total pore volume [cm^3/g]	Average pore diameter [nm]
LCO3	3.561	0.009	9.9
LCO5	21.584	0.056	10.3
LCO9	10.136	0.020	7.8

5. Summary

In recent years, perovskite materials have attracted the attention of materials scientists worldwide due to their exceptional catalytic and magnetic properties. In this study, the hydrothermal synthesis of LCO was investigated in detail, introducing a method for producing an exceptionally phase-pure crystalline LCO material. Optimization of synthetic parameters yielded optimal molar ratios, pH, and calcination temperature for the production of a nearly phase-pure perovskite, specifically a La:Co:citric acid ratio of 1:1.2:1, a pH of 8.5, and a calcination temperature of 750 °C.

Acknowledgement

This work was supported by the Czech Science Foundation under project number 25–17855K. The authors gratefully acknowledge the CzechNanoLab Research Infrastructure, supported by MEYS CR (LM2023051), for providing access to the equipment used in this study.

References

[1] Liu, D. (2021) In situ surface reconstruction on $LaCoO_{3-\delta}$ leads to enhanced hydrogen evolution reaction. *J. Alloys Compd.*, 891, 161754.
[2] Liu, Y. (2009) Study of $LaCoO_3$ as a cathode catalyst for a membraneless direct borohydride fuel cell. *J. Alloys Compd.*, 488, 204-207.
[3] Phadtare, D. (2019) Crystalline $LaCoO_3$ perovskite as a novel catalyst for glycerol transesterification. *Mol. Cat.*, 475, 110496.
[4] Neha (2022) Facile and template-free synthesis of nano-macroporous $LaCoO_3$ perovskite oxide for efficient diesel soot oxidation. *React. Kinet. Mech. Catal.*, 135, 1607-1620.
[5] Jayapandi, S. (2025) $LaCoO_3$ photocatalyst for environmental remediation and energy conversion applications. *Renew. Sustain. Energy Rev.*, 213, 115464.
[6] Natile, M.M. (2007) $LaCoO_3$: Effect of synthesis conditions on properties and reactivity. *Appl. Catal. B Environ.*, 72, 351-362.
[7] Berbenni, V. (2018) Synthesis of $LaCoO_3$ powder by a combined mechanical/thermal process. *Zeitschrift für Naturforschung B*, 73, 719-724.
[8] Parwaiz, S. (2025) Recent advances in $LaCoO_3$-based perovskite nanostructures for electrocatalytic and photocatalytic applications. *Crit. Rev. Solid State Mater. Sci.*, 51, 63-104.
[9] Vrankić, M. (2026) Impurity-modulated synthesis of $LaCoO_3$ perovskites: Linking synthesis parameters to crystal structure and cefixime photocatalytic performance. *J. Alloys Compd.*, 1065, 188107.
[10] Haas, O. (2004) Synchrotron X-ray absorption of $LaCoO_3$ perovskite. *J. Solid State Chem.*, 177, 1000-1010.
[11] Yao, S. (2019) $LaCoO_3$ acts as a high-efficiency co-catalyst for enhancing visible-light-driven tetracycline degradation of BiOI. *J. Am. Ceram. Soc.*, 103, 1709-1721.
[12] Ivanova, S. (2007) Microstructure of $LaCoO_3$ prepared by freeze-drying of metal–citrate precursors revealed by EPR. *J. Phys. Chem. Solids.*, 68, 168-174.
[13] Chagas, C.A. (2012) Alumina-supported $LaCoO_3$ perovskite for selective CO oxidation (SELOX). *Int. J. Hydrogen Energy*, 37, 5022-5031.
[14] Tepech-Carrillo, L. (2016) Preparation of Nanosized $LaCoO_3$ through Calcination of a Hydrothermally Synthesized Precursor. *J. Nanomater.*, 2016, 1-7.